SUPPORTING INFORMATION

Oxide-supported $IrNiO_x$ core-shell particles as efficient, cost-effective, and stable catalysts for electrochemical water splitting

Hong Nhan Nong,[a] Hyung-Suk Oh,[a] Tobias Reier,[a] Elena Willinger,[b] Marc-Georg Willinger,[b] Valeri Petkov,[c] Detre Teschner,*[b] Peter Strasser*[a]

[a] Prof. Dr., P., Strasser, Dr. H.S. Oh, H.N. Nong, T. Reier
The Electrochemical Energy, Catalysis, and Materials Science Laboratory, Department of Chemistry, Chemical Engineering Division, Technical University Berlin, Strasse des 17. Juni 124, TC 03, 10623 Berlin, Germany
E-mail: pstrasser@tu-berlin.de
[b] Dr. D. Teschner, Dr. E. Willinger, Dr. M.G. Willinger
Department of Inorganic Chemistry, Fritz-Haber-Institut der Max-Planck-Gesellschaft
Faradayweg 4-6, D-14195 Berlin, Germany
[c] Prof. Dr. V. Petkov
Department of Physics, Central Michigan University
Mt. Pleasant, MI 48859, USA

1. Chemicals and materials

Commercially available reagents were used in the synthesis of the $IrNi_x$ NPs as received. Nickel acetate tetrahydrate ($Ni(CH_3COO)_2.4H_2O$) was purchased from Alfa Aesar, and iridium (III) acetate ($Ir(CH_3COO)_3$) was purchased from Chempur. Oleic acid, oleylamine, 1,2-tetradecandiol, dichloromethane, dibenzyl ether, tetradecylamine, ammonium hydroxide aqueous solution, tin (IV) chloride ($SnCl_4$), and antimony (III) acetate ($Sb(CH_3COO)_3$) were purchased from Sigma Aldrich. Absolute ethanol was purchased from Merck.

Antimony tin oxide, nanopowder, particle size < 50 nm, ≥ 99.5% trace metal basis, surface area of 47 $m^2 g^{-1}$ was purchased from Sigma Aldrich. High surface area carbon Vulcan XC-72R carbon black, BET surface area ~250 $m^2 g^{-1}$ was purchased from Carbot.

2. Synthesis of mesoporous antimony doped tin oxide (Meso-ATO), Meso-ATO supported $IrNi_x$ bimetallic precursor nanoparticle alloys and supported pure Ir nanoparticle benchmarks

Synthesis of mesoporous antimony-doped tin oxide

1.28g of tetradecylamine (TDA, 95.0 %, Sigma Aldrich) was added to an ethanol solution (65 mL of ethanol, Sigma Aldrich,and 160 mL of ultrapure water) and the stirring was continued for 3 hours. 4.794 g of $SnCl_4$ (99.0%, Sigma Aldrich) and 0.48 g of $Sb(CH_3COO)_3$ (99.99%, Sigma Aldrich) were dissolved in 20ml of ethanol, followed by the introducing to TDA solution. After stirring for 1 hour, the mixture was added to 200 ml ammonium hydroxide solution (1.5 mmol L^{-1}) with stirring for 1 hour. The solution was refluxed for 72 hours at 80 °C and then cooled down to room temperature. The yellow precipitate was separated from the solution by centrifugation at 5000 rpm for 10 min and then washed and centrifuged 5 times. The as-prepared wet samples were transferred to a glass-lined stainless-steel autoclave and hydrothermally treated at 120 °C for 24 hr. In order to remove excess surfactant, the hydrothermal (HT) treated product was washed with ethanol for 5 times using centrifuge. Produced white powder was dried in a freeze dryer and then dry sample was calcined at 400°C for 3 hours in air.

Synthesis of $IrNi_x$ bimetallic nanoparticles supported on Meso-ATO

In a typical synthesis of $IrNi_3$NPs supported on Meso-ATO with about 20 wt.% of Ir, 0.45mmol of Ni (II) acetate tetrahydrate (98%, Alfa Aesar), 89 mg of Meso-ATO, 0.66 mmol of 1,2-tetradecanediol [90%,

Sigma Aldrich], 0.45 ml oleylamine [70%, Sigma Aldrich] and 0.45 ml oleic acid [99%, Alfa Aesar] were added to 45 ml dibenzyl ether [99%, Alfa Aesar] in a three-neck flask. The mixture was then heated to 80 °C and maintained at this temperature for 30 minutes under nitrogen flow to remove trace water. The temperature was then increased to 240 °C, and then 0.15mmol of $Ir(ac)_3$ [Chempur, 48% wt. Ir] was added to the reaction flask. The reaction solution was held at 240 °C for 1 hour and then cooled down to room temperature. 60 ml absolute ethanol [Merck] and 30 ml of toluene were added to the reaction mixture, then the mixture was sonicated for 30 minutes, after that, the NP solution was stirred overnight. The supported catalyst was washed with absolute ethanol several times and collected by centrifuge at 6500 rpm for 10 minutes. The slurry then was freeze dried for 20 hours. To remove the surfactants, supported $IrNi_x$ NPs were heated at 180 °C in synthetic air (25% Vol. of O_2 and 75% Vol. of N_2) for 2 hours. Then N_2 was purged into the furnace for 1 hour at 180 °C to remove O_2, after which the catalyst powders were further annealed at T°C in N_2 for 4 hours (T = 180, 250, 300, 400, and 500 °C). The real Ir weight loadings and Ni/Ir ratios in the as-prepared materials were then evaluated by ICP-OES measurements.

Synthesis of supported pure Ir nanoparticle benchmarks

In particular, to synthesize Ir nanoparticles supported on carbon, 0.2 mmol of $Ir(CH_3COO)_3$ was dissolved in 40 mL of a 0.15 M solution of sodium hydroxide in ethylene glycol. The solution was degassed with nitrogen for 5 min and then heated under nitrogen flow, stirring and reflux to 160 °C and kept at this temperature for 30 min. Afterwards the reaction mixture was cooled down rapidly. 192.2 mg of carbon were suspended in 30 ml of ultrapure water and 5 ml of concentrated CH_3COOH by sonication for 10 min, and then Ir nanoparticle solution was added to the mixture, followed by stirring for 24 hours. The suspension was then centrifuged (10 min, 7700 rpm) and washed several times with ultrapure water. The collected Ir/support slurry was freeze dried for 20 hours. The received powder washeat treated at 250 °C in N_2 atmosphere to remove remained organic substances. For Ir nanoparticles supported on com.-ATO, all steps were carried out similar to Ir/C, with an exception that the ATO powder was added to the $Ir(CH_3COO)_3$ solution before reaction starts.

3. Microscopic and spectroscopy characterization

Powder XRD. Powder XRD profiles were measured in Bragg−Brentano geometry in a D8 Advance X-ray diffractometer (Bruker AXS) using a Cu Kα source, variable divergence slit, and a position sensitive device as detector. Data were collected in a 2θ range of 20° to 95° with an increment of 0.05°, a measuring time of 5 s per step, and a sample rotation rate of 15 rotations per minute.

ICP. ICP-OES compositional analysis was performed using a 715-ES-inductively coupled plasma (ICP) analysis system (Varian). The standard concentrations were 1, 2, 4 and 6 ppm for Ir and Ni. The chosen wavelengths for concentration determination were 212.681, 224.268, 236.804, 254.397, and 263.971 nm for Ir and 216.555, 221.648, 222.295, 227.021, 230.299, and 231.604 nm for Ni.

TEM. TEM micrographs were acquired using a FEI TECNAI G^2 20 S-TWIN equipped with LaB6 cathode and GATAN MS794 P CCD camera. The microscope was operated at an acceleration voltage of 200 kV. The catalyst powders were suspended in ethanol; then the suspension was pipetted onto a carbon coated copper grid (400 mesh, Plano).

HAADF-STEM and elemental mapping. High-resolution scanning transmission electron microscopy (STEM) was performed using aJeol JEM-ARM200CF. The JEM-ARM200CF is a probe aberration corrected 200kV STEM/TEM with a cold field emission source with 0.35eV energy resolution. For HAADF imaging at 200kV this instrument has a resolution of less than 0.08nm.

XPS. $IrNi_x$ catalysts were characterized by X-ray photoelectron spectroscopy at the ISISS beamline of the synchrotron facility BESSY of the Helmholtz-Zentrum Berlin. A detailed description of the setup can be found elsewhere.[1] Samples were mounted onto a sapphire sample holder and introduced into the spectrometer. XPS experiments were carried out at room temperature (RT) in ultra-high vacuum (UHV). To calculate elemental ratios, the peak areas of Ir4f, Ni2p and O1s were corrected considering the photon flux and tabulated cross sections.[2]

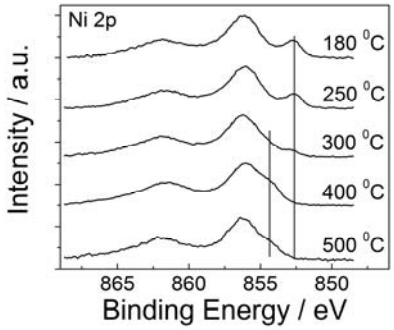

Figure S1: Ni2p XPS spectra of $IrNi_x$ nanoparticles supported on mesoporous ATO ($IrNi_x$/Meso-ATO-T) annealed at different temperature T (T = 180, 250, 300, 400, 500 °C). XPS spectra were measured at kinetic energy of 550 eV.

In the XPS Ni2p(3/2) spectra of the $IrNi_x$/Meso-ATO-T (Fig. S1), the most intense Ni2p(3/2) line is situated at ~856 eV, with the satellite at ~862 eV, which is similar to that observed before with Ir-Ni NPs on carbon.[3] Although the binding energy is much up-shifted compared to crystalline NiO, the shape of Ni2p with the strong satellite and characteristic satellite main peak separation suggest a Ni^{2+} state. The low-T annealed samples reveal a clear low binding energy component at ~852.6 eV, which is characteristic of metallic Ni. Thus after low-T annealing, the samples contain an alloyed metallic Ir-Ni phase. For samples annealed at 400 and 500 °C, there appears a low binding energy oxidized Ni component, which binding energy fits well to crystalline NiO.

Table S1: Elemental ratios of pristine PA-$IrNi_x$/ATO-T annealed at different temperature and $IrNiO_x$/Meso-ATO-180 derived from XPS (photoelectron kinetic energy: 550 eV) and/or ICP-OES.

Samples	Ni/Ir		Ir/ (Sb+Sn+O+Ni)	Ir/ (Sn+Sb)	O/ (Sb+Sn)	Sb/Sn	(Ir+Ni)/ (Sb+Sn)
	XPS	ICP-OES	ICP-OES	XPS	XPS	XPS	XPS
Meso-ATO	-	-	-	-	1.8	0.14	-
$IrNi_x$/Meso-ATO-180	4.5	3.3	0.193	0.11	1.8	0.12	0.5
$IrNi_x$/Meso-ATO-250	5.0	3.4	0.175	0.12	1.8	0.14	0.7
$IrNi_x$/Meso-ATO-300	11.0	3.8	0.160	0.04	1.7	0.1	0.5
$IrNi_x$/Meso-ATO-400	16.6	3.6	0.167	0.035	1.7	0.09	0.6
$IrNi_x$/Meso-ATO-500	9.4	3.7	0.155	0.03	1.8	0.1	0.3

High-energy synchrotron XRD measurements were carried out at beamline 11-ID-C at the Argonne National Laboratory using X-rays with wavelength of 0.11165 Å. Scattering intensities were collected with

large area detector. Samples, including supported NPs and pure ATO were inside glass capillaries 1.5 mm in diameter. Raw XRD data were corrected for air (measured separately), instrumental (measured separately) and ATO support (measured separately) scattering, converted into absolute (electron) units and then Fourier transformed into atomic PDFs. Note as obtained PDFs largely reflect atomic correlations/atomic-scale structure in Ir-Ni NPs since the contribution from ATO support has been eliminated during raw data processing.

Experimental atomic PDFs were approached with simple models based on/constrained to fcc-type structure/lattice occurring both with bulk Ni and Ir. Within this simplistic model approximation, atoms have to occupy identical sites/vertices of an fcc-type lattice and so are assigned appropriately averaged, (3*Ni + 1*Ir)/4, scattering power for x-rays. Reported fcc-lattice parameters were obtained by the fitting model computed against experimental PDFs. Note so obtained fcc-lattice parameters reflect the whole set of characteristic interatomic distances in the respective NPs. Yet, without any model assumptions, individual interatomic distances such as radii of first atomic coordination spheres/average first atomic pair distances can be extracted directly from the experimental PDFs.

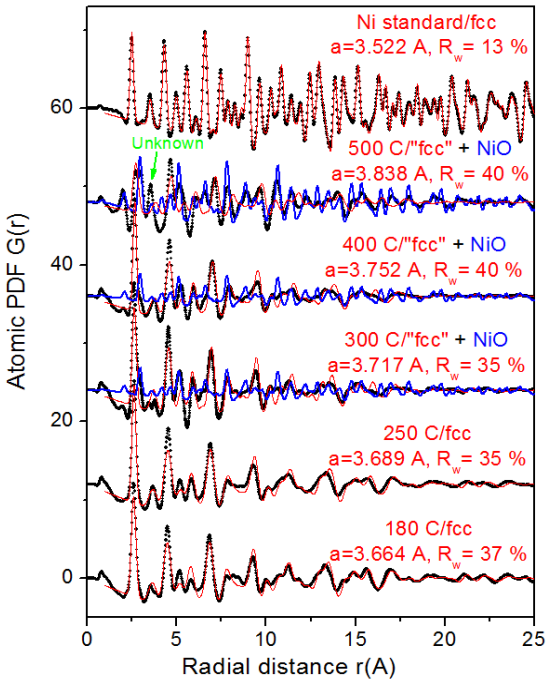

Figure S2. Experimental (symbols) and model (solid lines) atomic PDFs for $IrNi_x$/Meso-ATO. Models feature fcc-type (line in red) metallic alloy and NiO nanophase (line in blue). Refined "fcc-lattice parameters" are given by each data set (in red). Respective fcc model agreement/fit quality factors (R_w) are also given (in %).

Atomic PDFs models for PA-$IrNi_x$/Meso-ATO-T (Fig S2) feature fcc-type (red line) metallic alloy and NiO nanophase (blue line). NPs treated at 180 °C and 250 °C are metallic nanoalloys of fcc-type structure, though the fcc structure is somewhat "distorted". NPs treated at 500 °C are completely phase segregated into Ir-based metallic nanophase and NiO nanophase. Surprisingly, no signatures of IrO_2 nanophase are seen, though XPS results indicated that we have Ir oxide, which might be due to similar interatomic distances in NiO and rutile IrO_2. Beside, a third, unidentified nanophase is clearly present in the sample treated at 500 °C.

Hollow core-shell and solid core-shell nanoparticles

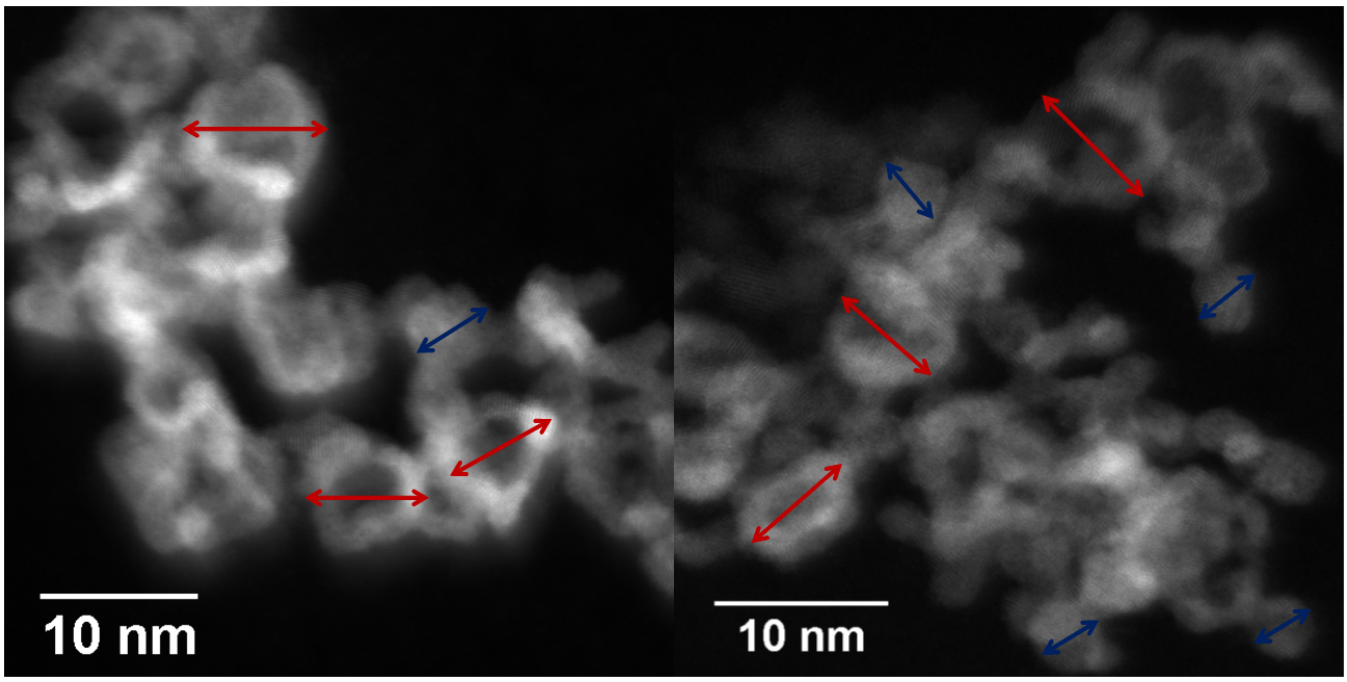

Figure S3. HAADF-STEM images of hollow core-shell (red arrows) and solid core-shell (blue arrows) nanoparticles.

HAADF STEM images (Figure S3) were used to estimate the size distribution of the core-shell particles. Due to the anisotropic shape of the nanoparticles, the measured size distribution is affected by the orientation of the particles. Nevertheless, the size distribution of the larger hollow particles is quite narrow and in the range of 7 to 11 nm (red arrows). For the small Ni rich particles, the sizes are below 4.5 nm (see blue arrows). In fact, the size of the hollow and solid core-shell nanoparticles did not change during electrochemical treatment.

4. Electrochemical measurements

Electrochemical setup

Electrochemical experiments were performed in a three-compartment glass cell with a rotating disk electrode (RDE, 5 mm in diameter of glassy carbon - GC, Pine Instrument) and a potentiostat (Biologic) at room temperature. A Pt-mesh and a Hg/Hg_2SO_4 electrode (in saturated K_2SO_4) were used as counter electrode and reference electrode, respectively. All electrochemical measurements were carried out in N_2-saturated 0.05M H_2SO_4 and repeated on three catalyst films for each catalyst.

Working electrode preparation

To prepare the working electrode, a certain amount of catalyst was suspended in 2.490 mL of ultrapure water (Millipore, 18 MΩ), 2.490 mL of isopropanol and 20 µL of 5 wt% Nafion solution with sonication for 30 minutes to form a uniform ink. Ten µL of the ink was pipetted onto pre-polished and cleaned GC electrode and dried at 60 $^{\circ}$C for 7 minutes in air, resulting in a uniform catalyst thin film. The amount of catalysts was calculated in order to get the final film on GC electrode containing 10.2 $\mu g_{Ir}.cm^{-2}$. All potentials reported in this paper were normalized with respect to the reversible hydrogen electrode (RHE).

Electrochemical protocol for synthesizing $IrNiO_x$ core-shell nanoparticles

From our previous study,[3] directly oxidized core-shell *$IrNiO_x$* nanoparticles showed better OER activity than stepwise oxidized NPs, therefore, we utilized direct electrochemical oxidation protocol for our $IrNi_x$/Meso-ATO-T catalysts. In particular, the precursor alloy nanoparticles were dealloyed and oxidized by applying potential cycling from +0.05 V to +1.5 V vs. RHE for 50 cycles with a scan rate of 500 mVs^{-1}.

The characteristic $Ir^{III/IV}$ redox couple is usually used to estimate the molar amount of catalytically active Ir atoms for Ir catalysts.[3] The $Ir^{III/IV}$ wave is decreased with increasing annealing temperature, indicating the decrease of number of active sites (Fig. S4a).

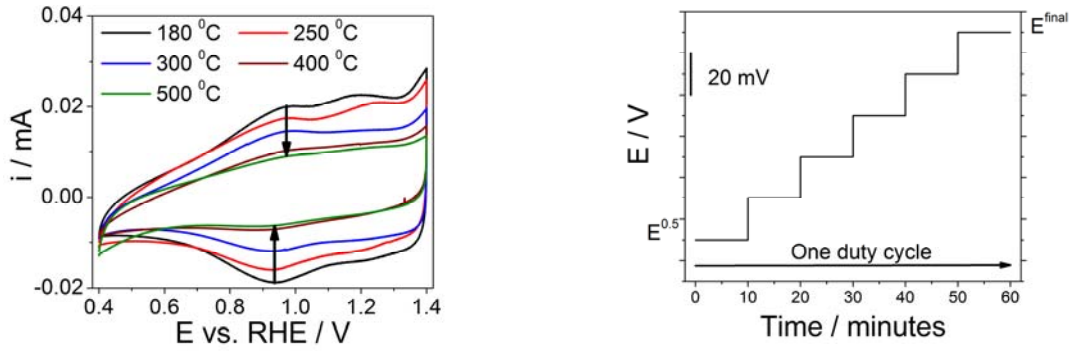

Figure S4. a) Ir redox peak of $IrNiO_x$ core-shell supported on mesoporous ATO annealed at different temperature T, (T = 180, 250, 300, 400, 500 ^{0}C), and b) one duty cycle of the durability test under stepwise load increase.

Electrocatalytic activity of core-shell $IrNiO_x$/Meso-ATO-T catalysts for the oxygen evolution reaction

The electrochemical catalytic activity of the Ir-Ni@IrO_xNPs was recorded during cyclic sweep voltammetry between+1.0 V to +1.8 V with a scan rate of 5 mV s^{-1} under electrode rotation of 1600 rpm. PEIS (Potential Electrochemical Impedance Spectroscopy) was carried out before each OER measurement for IR correction. The Ir-mass based OER activity was evaluated at 0.28 V overpotential (+1.51 V vs. RHE) taking the averagecurrent density values of the IR-corrected and capacity-corrected anodic and cathodic scans. The capacitance currents were evaluated by the mean value of the current in the potential range of 1.0 to 1.23 V, where no faradaic process takes place.

Stability test of core-shell $IrNiO_x$/Meso-ATO-180 catalyst

Chronopotentiometric measurements. The catalytic stability was tested for the pure Ir/C and Ir/com.-ATO-180 °C and directly oxidized core-shell $IrNiO_x$/Meso-ATO by chronopotentiometry technique, in which current density was held at 1 mA $cm^{-2}$for a period of 20 hours and corresponding potential was recorded.

Duty cycle measurements. In order to test the stability of the catalysts under conditions similar to working conditions of PEM electrolyzers, we used a duty cycle protocol (Figure S4b), in which the potential was first kept at $E^{0.5}$ (where current density reached 0.5 mA cm^{-2}) for a period of 10 minutes, then increased by 20 mV and kept at the new value for 10 minutes. This increasing step was repeated for 5 times until the last holding potential E^{final} equaled to $E^{0.5}$ + 100 mV. This allows the catalysts undergo similar conditions as in the operating conditions of an electrolyzer. The process from the holding potential of $E^{0.5}$ to E^{final} was then called one duty cycle. The duty cycle was repeated for 5 times, after each duty cycle, the OER activity was tested by cyclic voltammetry technique. The potential at which a current

density of 1 mA cm^{-2} after each duty cycle was presented in Figure 4d, cycle number 0 indicates the first OER tests before duty cycles.

References

(1) Knop-Gericke, A.; Kleimenov, E.; Hävecker, M.; Blume, R.; Teschner, D.; Zafeiratos, S.; Schlögl, R.; Bukhtiyarov, V. I.; Kaichev, V. V.; Prosvirin, I. P.; Nizovskii, A. I.; Bluhm, H.; Barinov, A.; Dudin, P.; Kiskinova, M. In *Advances in Catalysis*; Bruce, C. G., Helmut, K., Eds.; Academic Press: 2009; Vol. Volume 52, p 213.

(2) Yeh, J. J.; Lindau, I. *Atomic Data and Nuclear Data Tables***1985**, *32*, 1.

(3) Nong, H. N.; Gan, L.; Willinger, E.; Teschner, D.; Strasser, P. *Chemical Science***2014**, *5*, 2955.